# Terahertz Imaging System based on Superconducting Integrated Receiver.

Ozhegov R.V.[1,2], Gorshkov K.N[2]., Smirnov K.V.[1], Gol'tsman G.N.[2], Filippenko L.V.[3], Koshelets V.P.[3]

1. Joint Stock Company "Superconducting Nanotechnologies", Rossolimo st., 5/22, Moscow, Russia.
2. Moscow State Pedagogical University, M. Pirogovskaya st., 29, Moscow, Russia.
3. Institute of Radio Engineering and Electronics (IREE), Moscow, Russia.

The development of terahertz imaging instruments for security systems is on the cutting edge of terahertz technology. We are developing a THz imaging system based on a superconducting integrated receiver (SIR). An SIR is a new type of heterodyne receiver based on an SIS mixer integrated with a flux-flow oscillator (FFO) and a harmonic mixer which is used for phase-locking the FFO. Developing an array of SIRs would allow obtaining amplitude and phase characteristics of incident radiation in the plane of the receiver. Employing an SIR in an imaging system means building an entirely new instrument with many advantages compare to traditional systems: i) high temperature resolution, comparable to the best results for incoherent receivers; ii) high spectral resolution allowing spectral analysis of various substances; iii) the local oscillator frequency can be varied to obtain images at different frequencies, effectively providing "color" images; iv) since a heterodyne receiver preserves the phase of the radiation, it is possible to construct 3D images. The paper presents a prototype THz imaging system using an 1 pixel SIR. We have studied the dependence of the noise equivalent temperature difference (NETD) on the integration time and also possible ways of achieving best possible sensitivity. An NETD of 13 mK was obtained with an integration time of 1 sec a detection bandwidth of 4 GHz at a local oscillator frequency of 520 GHz. An important advantage of an FFO is its wide operation range: 300-700 GHz.

Rapid development of terahertz technologies has prompted a research into the possibility of using terahertz receivers in areas other than purely scientific. Among these, of great interest is the feasibility of building terahertz imaging systems for security applications. As of this writing, the systems actively in use are based on acoustic, magnetic, and electromagnetic principles, for example, an acoustic detector of hard substances or a magnetic detector of metal objects. However, they are ineffective for detection and recognition of potentially dangerous nonmetallic objects hidden under clothes or in the mail, such as plastic weapons, explosives, and drugs. The terahertz region of the spectrum could provide safe, fast imaging technologies that can detect hidden objects under clothes no matter what material they are made from.

Currently there are a great number of imaging systems that differ from each other mainly in the frequency range, which determines the quality of the images and also the feasibility of recognition of hidden objects. For example, infrared (IR) imaging systems are ineffective in some cases because of strong absorption of IR radiation in the clothes, human tissue, and atmosphere. At radio frequencies, penetration is better, but in this case the spatial resolution, determined by the wavelength, is much worse. The solution lies in the middle, at terahertz frequencies, where good penetration combined with good spatial resolution allows recognition of hidden objects, including weapons, explosives, and drugs.

Currently there are several commercial imaging systems (for example [1 ,2]). When describing the capabilities of modern imaging systems it is necessary to formulate the basic requirements they should meet:

- Possibility of remote imaging;
- Possibility of passive imaging (this is especially important in the systems where, firstly, the observer must not be visible and secondly, the use of active imaging may cause health problems);
- Possibility of detecting object hidden under clothes or in luggage;
- Possibility of determining the material the studied object is made of.

It should be noted that all modern commercial imaging systems meet only several of the above requirements. We believe heterodyne receivers have a great potential of becoming the receivers of choice in imaging systems because not only do they meet all the aforementioned requirements but also have excellent spatial and temporal resolution. Employing an SIR in an imaging system means building an entirely new instrument with many advantages compare to traditional systems:

- high temperature resolution, comparable to the best results for incoherent receivers;
- high spectral resolution allowing spectral analysis of various substances;

- the local oscillator frequency can be varied to obtain images at different frequencies, effectively providing “color” images;
- since a heterodyne receiver preserves the phase of the radiation, it is possible to construct 3D images.

The temperature resolution of a heterodyne receiver is given by [3]:

$$NETD = \alpha T_N \sqrt{1 + \frac{T_S}{T_N} + \frac{3}{8}\left(\frac{T_S}{T_N}\right)^2} \frac{1}{\sqrt{B_H \Delta t}}, \qquad (2)$$

where $T_N$ is the receiver noise temperature, $T_S$ is the antenna temperature associated with the object, $B_H$ is the IF bandwidth, and $\Delta t$ is the integration time. The factor $\alpha$ depends on the receiver type and is of order unity. Most often a different expression is used:

$$NETD = \alpha T_N \frac{1}{\sqrt{B_H \Delta t}}, \qquad (3)$$

which follows from (2) if $T_S \ll T_N$. Provided that the integration time is fixed, the NETD can be improved by means of decreasing the receiver noise temperature and increasing its IF bandwidth. Unlike an incoherent receiver, a heterodyne receiver with a reasonably high sensitivity is capable of measuring transmission and absorption spectra of an object and so potentially affords determination of its chemical composition.

We decided to develop and build a passive imaging system based on a heterodyne receiver. At terahertz frequencies SIS (Superconductor-Insulator-Superconductor) and HEB (Hot-Electron Bolometer) mixers currently demonstrate the best performance. Below 1.4 THz SIS mixers offer a lower noise temperature and better stability compared to HEB mixers. Above frequency 0.9 THz HEB mixers performance degrades due to the energy gap effect.

At the heart of our system is a superconducting integrated receiver (SIR) comprising, on a $4\times4\times0.5$ mm$^3$ chip, a low-noise SIS mixer integrated with a flux-flow oscillator (FFO), used as a local oscillator (LO), and a harmonic mixer for phase-locking the FFO [4-6]. The SIR does not require any sophisticated equipment and can be operated with the use of only dc power supply Currently, the best SIRs have a noise temperature that does not exceed 200 K at LO frequencies of 500-700 GHz, and FFOs can be swept in the range 300-800 GHz with the width of the line not greater than 1 MHz.

A schematic of the experimental setup used to measure the NETD is shown in Fig. 1. The SIR is mounted in the focus of an elliptical lens which is installed into a mixer block carrying two magnetic screens. The screens are made of permalloy and lead and protect the SIR from external magnetic fields. Such isolation is necessary because the FFO is extremely sensitive to any variation of a magnetic field. The mixer block is mounted on the cold plate of a liquid helium cryostat. The SIR is remotely controlled. The NETD was measured at 520 GHz, where the receiver had a noise temperature of 170 K over within the IF range 4-8 GHz. A more detailed discussion of the choice of the operating regime may be found in [8].

We chose an Ecosorb load as a signal source with a variable temperature. The signal was modulated at 400 Hz by a chopper whose blades were also covered with an absorbing material at room temperature. The output signal was fed to a square-law detector. Fig. 2 shows the voltage at the output of the detector as a function of time for different temperatures of the load. The NETD was determined from the standard deviation of the detector voltage. For the curve corresponding to a temperature differential of 170 K the NETD was found as ~150±30 mK. For the other curve, corresponding to the temperature differential of 2 K, the NETD was found as ~13±2 mK.

NETD measured in the experiment shows good agreement with the theoretical prediction. The difference between the two experiments can be explained as follows (see Fig. 2). We have an amplitude modulated signal

$$U(t) = U_0 (1 + \delta U \sin(\Omega t)), \tag{4}$$

where $\Omega$ is angular modulation frequency, $U_0$ is the signal mean, and $\delta U$ is the modulation depth (this factor corresponds to the relative magnitude of the useful signal).

Suppose now that the receiver has an instability caused, for example, by instabilities in the bias of the IF amplifiers or the mixer operating point, or fluctuations of the LO drive. There may other causes but we will not discuss them yet, and assume for simplicity that all the instabilities are caused by the receiver gain:

$$G(t) = G_0 (1 + \delta G \sin(\omega t)), \tag{5}$$

where $G_0$ is the mean value of the gain (including the mixer conversion efficiency and the IF amplifier gain) and $\delta G$ is its modulation depth and determines the magnitude of gain fluctuations. As a result, the output of the lock-in amplifier is

$$U_{OUT}(t) = G(t) U(t) \sin(\Omega t). \tag{6}$$

When expanding Eq. (6) we should allow for the lowpass filter which determines the integration time of the lock-in amplifier. Thus we neglect all the harmonics with frequencies greater than zero and have:

$$U_{OUT}(t) = \frac{G_0 U_0}{2} \left( \delta U + \delta G_{\omega=\Omega} \cos(\Omega - \omega)t + \delta U \delta G_{\omega=0} \sin(\omega t) \right), \tag{7}$$

In Eq. (7), the first term in the curly brackets is the useful signal, and the other two describe the effect of the gain fluctuations. We should note that in a real experiment the power spectral density of fluctuations can be quite broad. The contribution of the second term in Eq. (7) can be significant at frequencies close to the modulation frequency. To suppress this spurious contribution the modulation frequency should be increased thereby avoiding 1/f noise present in the IF chain. During the experiment the modulation frequency was 400 Hz. Such a modulation frequency was found sufficient to achieve the best NETD.

The contribution of the third term is significant when fluctuations vary slowly in time (the corresponding frequency is close to zero). In this case the magnitude of the spurious signal is proportional to $\delta U$. The contribution of the third term is shown by the data in Fig. 2. The standard deviation of the signal is a function of the temperature difference at the receiver input. As this difference is decreases so does the standard deviation. Thus when the temperature difference was decreased from 170 K to 2 K the receiver sensitivity improved by more than a factor of 10. The best sensitivity measured in the experiments was 13±2 mK. This value of NETD is a best value for the THz mixers. This fact allows SIR to take a special place among THz receivers applied in systems of technical sight.

To demonstrate the capabilities of the SIR to produce terahertz images we used a mechanical scanner with a system of Teflon lenses to focus the radiation onto the chip. As the test object we chose a five-pointed star made from a piece of Ecosorb ~50 mm in diameter and held at room temperature. To imitate the detection of an object against a human body we used a larger piece of Ecosorb held at a temperature 16 K above that of the star in front of it (a temperature differential of 16 K is the average difference between room temperature and human body temperature). The image obtained with the use of the SIR is shown in Fig. 3. The spatial resolution in this case is ~2 mm. Performance of the SIR the best (spatial resolution, noise equivalent temperature difference, Possibility of determining the material the studied object) in comparison with other commercially accessible receivers.

Reference:


1. http://www.thruvision.com/
2. http://www.teraview.co.uk
3. Esepkina N. A., Korol'kov D. V., Pariyskiy Yu. N. Radiotelescopes and radiometers. 1973. //in Russian.
4. Koshelets V.P., Shitov S. V., Filippenko L. V., et al. // Appl. Phys. Lett. 1996. V. 68. № 9. P. 1273.
5. Koshelets V.P., Shitov S. V. // Supercond. Sci. Tech. 2000. V. 13. P. R53.
6. Gert de Lange, Dick Boersma, Johannes Dercksen, Pavel Dmitriev, Andrey B. Ermakov, Lyudmila V. Filippenko, Hans Golstein, Ruud W.M. Hoogeveen, Leo de Jong, Andrey V. Khudchenko, Nickolay V. Kinev, Oleg S. Kiselev, Bart van Kuik, Arno de Lange, Joris van Rantwijk, Alexander S. Sobolev, Mikhail Yu. Torgashin, Ed de Vries, Pavel A. Yagoubov, and Valery P. Koshelets, "Development and Characterization of the Superconducting Integrated Receiver Channel of the TELIS Atmospheric Sounder", Supercond. Sci. Technol. vol. 23, 045016 (8pp), (2010).

Figure captions

Fig. 1. A block diagram of the SIR.

Fig. 2. The output signal stability for various levels of the input signal. As the intensity of the input signal is decreased the NETD goes down and reaches the values predicted theoretically.

Fig. 3. A photograph of the object (five-pointed star) -- on the left, and its terahertz image obtained with the SIR --on the right. The object diameter is ~50 mm.

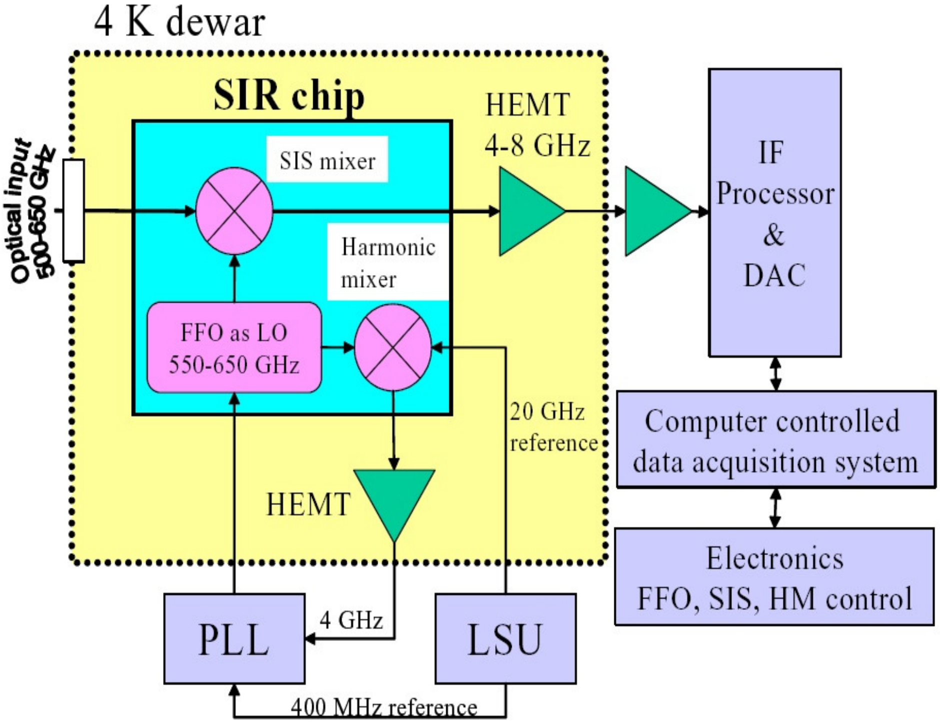

4 K dewar
SIR chip
Optical input
500-650 GHz
SIS mixer
Harmonic
mixer
FFO as LO
550-650 GHz
HEMT
4-8 GHz
20 GHz
reference
HEMT
IF
Processor
&
DAC
Computer controlled
data acquisition system
Electronics
FFO, SIS, HM control
PLL
4 GHz
LSU
400 MHz reference

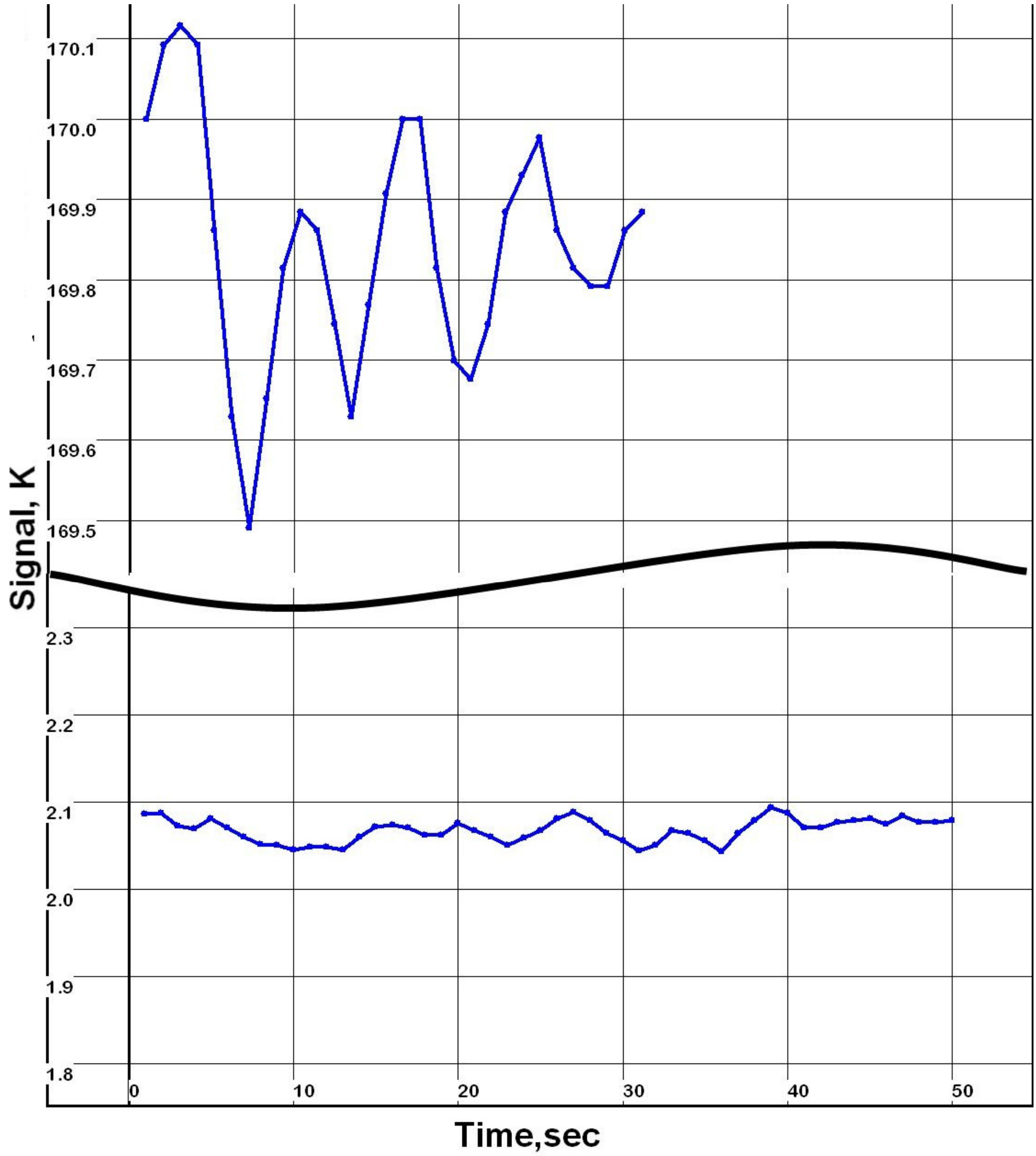

Signal, K
170.1
170.0
169.9
169.8
169.7
169.6
169.5
2.3
2.2
2.1
2.0
1.9
1.8
0
10
20
30
40
50
Time,sec